INTERNATIONAL JOURNAL OF EXPLORING EMERGING TRENDS IN ENGINEERING
Peer-Reviewed, Refereed, Indexed and International Journal, https://ijoeete.com/
|ISSN No. 2394-0573 |Volume: 9, Issue: 01 | January - June 2022

SYNTHESIS, CHARACTERIZATION AND ANTIMICROBIAL ACTIVITY OF DIVALENT TRANSITION METAL COMPLEXES OF HYDRAZINE AND TRIMESIC ACID

[1] Kartik Pundir, [2]Dr. Shiv Brat Singh
[1]Research Scholar, [2]Supervisor
[1-2] Department of Chemistry, CMJ University, Meghalaya, India

Abstract

In this study, the synthesis, characterization, and antimicrobial activity of divalent transition metal complexes with hydrazine and trimesic acid are explored. The complexes of $M(Htma)(N_2H_4)_2$ (where M = Mn, Co, Ni, Cu, and Zn) were synthesized using metal nitrate hydrates, trimesic acid (benzene-1,3,5-tricarboxylic acid), and hydrazine hydrate. The synthesized complexes were characterized through various spectroscopic techniques such as FT-IR, UV-Vis, EPR, Raman, X-ray diffraction, and thermal analysis. The electronic spectra indicated octahedral coordination for most of the metal ions, while the IR spectra confirmed the coordination modes of carboxylate and hydrazine groups. The compounds exhibited notable antimicrobial activity, with varying efficiencies against different bacterial strains. These results suggest the potential of these complexes for applications in antimicrobial treatments.

Keywords: Trimesic acid, transition metal complexes, hydrazine, antimicrobial activity, FT-IR, EPR, UV-Vis, X-ray diffraction.

1. Introduction

Exploration of coordination complexes has enticed the focus of numerous investigators globally due to their captivating molecular assemblies united by influences such as metal–ligand coordination, stacking connections, and hydrogen bonding. [uno,dos] These coordination compounds are anticipated to discover utilities as novel materials with captivating photophysical, photochemical, catalytic, sensing, magnetic and electronic characteristics.[trio, quartet] Hydrazine, the most modest diamine even after getting protonated as N2H5+, demonstrates its capability to associate with numerous metal ions and creates various salts with mineral as well as carboxylic acids. The chemistry of hydrazine is noteworthy because of its capacity to create diverse mixed-ligand complexes with transition metals, whose stability and other characteristics alter significantly based on the cations as well as the anions.[quintet, sextet] Thermal disintegration investigations of metal carboxylates with hydrazine as co-ligand are capturing the interest of scientists, as they function as forerunners for the creation of nanoparticle oxide substances and metal carbonates through uncomplicated pyrolysis response.[septenary–nonary] Neutral hydrazine associates with the metal ions primarily in two distinct ways, namely, either monodentate or bidentate bridging ligand (not merely bidentate to a metal ion). In the existence of carboxylic acids, hydrazine may bind with metal ions as hydrazinium cation since hydrazine subsists as hydrazinium cation in acidic circumstances. The essence of the intricate formed (impartial hydrazine or hydrazinium ion) relies on the abundance of hydrazine, acidity of the reaction mixture, and characteristic of the metallic ion. Hydrazinium (mono-acidic hydrazine) complexes are thermally less durable than neutral hydrazine complexes, but they are structurally intriguing.

Trimesic acid, also known as benzene-1,3,5-tricarboxylic acid, is a compound derived from benzene that has three carboxylic acid groups. Tricarboxylates of Yttrium (III) and rare earth elements (III) were synthesised and characterised.The user's text is "[10]". Two newly synthesised transition metal–organic frameworks, one with zinc (Zn) and the other with cadmium (Cd), were prepared and analysed. The frameworks were constructed using benzene-1,3,5-tricarboxylic acid and a radiant complex of terbium (Tb) and trimesic acid (TMA).The numbers are eleven and twelve. The three newly synthesised metal-trimesate compounds are denoted as [Cd3(TMA)2(H-PRZ)(H2O)3(OH)].The compounds mentioned are H2O (1), Cd2Na2(TMA)2(H2O)4 (2), and [Cd2Co(TMA)2(H2O)4].The solid state fluorescence emissions of ·2H2O (3) at ambient temperature were observed due to its diverse coordination structures.The user's text is "[13]". The previously given knowledge motivated us to synthesise new compounds by combining certain divalent transition elements (Cobalt, Nickel, Copper, Manganese, and Zinc) with 1,3,5-benzenetricarboxylic acid (Trimesic acid, H3tma) and hydrazine. Figure 1 demonstrates the many possible synchronisation techniques

INTERNATIONAL JOURNAL OF EXPLORING EMERGING TRENDS IN ENGINEERING
Peer-Reviewed, Refereed, Indexed and International Journal, https://ijoeete.com/
|ISSN No. 2394-0573 |Volume: 9, Issue: 01 | January - June 2022

between benzene tricarboxylic acid and metallic ions.

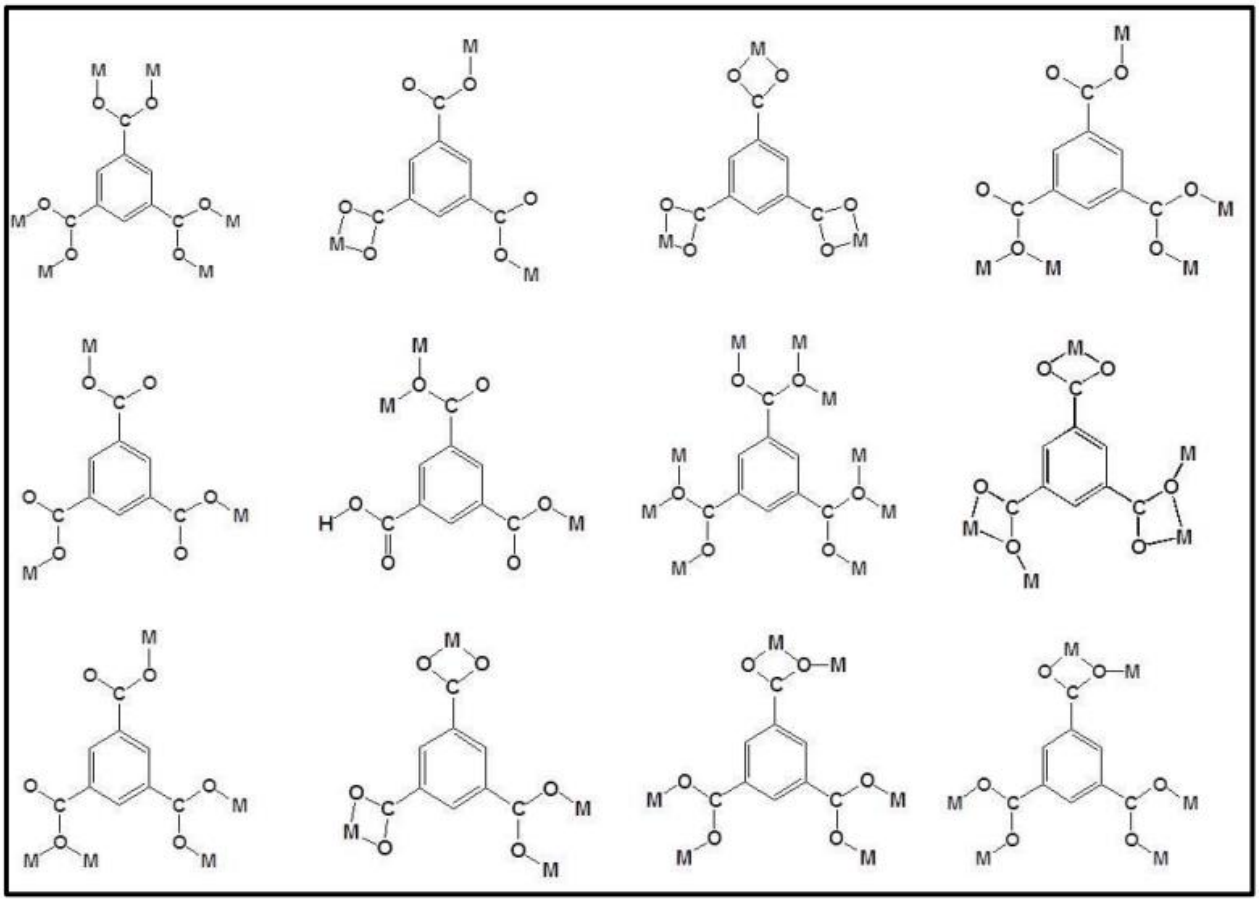

Source http://dx.doi.org/10.1016/j.jscs.2017.05.012

Fig. 1. Coordination fashions of trimesic acid (TMA).

2. Experimental section

2.1 Materials and methods

The substances utilised for the amalgamation and diverse physico-chemical methodologies employed in this study (Analytical, ESI-mass, electronic, FT-IR, Raman, EPR and EDX spectral, powder X-ray diffraction, TG–DTA, SEM and antimicrobial activities) are deliberated in Chapter II.

2.2 Synthesis of M(Htma)(N2H4)2, where M = Mn, Co, Ni, Cu and Zn

Benzene-1,3,5-tricarboxylic acid (0.735 g, 0.0035 mol) was added to a 50 mL aqueous solution of hydrazine containing 0.171 mL (0.0035 mol) of pure (99.5%) hydrazine hydrate. The mixture was heated on a water bath at 90 °C with stirring until a translucent solution was obtained. The matching metal nitrate (0.0035 mol, pH 5) was slowly added to an aqueous solution and stirred continuously. The mixture was then refluxed at 80 °C for 12 hours. Manganic acetate tetrahydrate was used in the case of Mn. The volume of the mixture was reduced to about 20 mL by concentrating it over a water bath at a temperature of 80–90 °C. Subsequently, it was allowed to cool for 6 hours, during which time the resulting synthesis was entirely precipitated. The complex chemical was separated using filtering, washed with purified water, ethanol, and hydrocarbon, and then allowed to air dry.

3. Results and discussion

INTERNATIONAL JOURNAL OF EXPLORING EMERGING TRENDS IN ENGINEERING
Peer-Reviewed, Refereed, Indexed and International Journal, https://ijoeete.com/
|ISSN No. 2394-0573 |Volume: 9, Issue: 01 | January - June 2022

The synthesis of manganese, cobalt, nickel, copper, and zinc compounds was achieved by combining aqueous solutions of the respective metal nitrate hydrate, benzene-1,3,5-tricarboxylic acid, and hydrazine hydrate.

$$M(NO_3)_2.6H_2O + C_6H_3(COOH)_3 + 2N_2H_4.H_2O \rightarrow$$

$$[M(C_6H_3(COO)_2COOH)(N_2H_4)_2] + 2HNO_3 + 8H_2O \rightarrow \textbf{(1)}$$

where M = Co, Ni, and Zn.

$$Cu(NO_3)_2.3H_2O + C_6H_3(COOH)_3 + 2N_2H_4.H_2O \rightarrow$$

$$[Cu(C_6H_3(COO)_2COOH)(N_2H_4)_2] + 2HNO_3 + 5H_2O \rightarrow \textbf{(2)}$$

$$Mn(CH_3COO)_2.4H_2O + C_6H_3(COOH)_3 + 2N_2H_4.H_2O \rightarrow$$

The analytical data for the prepared compounds may be found in Table 1. The newly prepared metal hydrazine carboxylates have low solubility in water, alcohol, and other organic solvents, but are soluble in a mixed solvent of methanol and acetylacetone. The formulations of these complexes were determined based on the elemental composition (CHN), as well as the presence of hydrazine and metal elements. Please refer to Table 1 for further details. In order to further confirm the proposed chemical formula of the complexes, mass spectroscopy investigations were performed. Figure 3 displays the mass spectra of the Cobalt(II), Nickel(II), Copper(II), Manganese(II), and Zinc(II) complexes.Kindly rephrase your language or provide more context to facilitate my comprehension of your request. The mass spectra of the Cobalt(II), Nickel(II), Copper(II), Manganese(II) and Zinc(II) complexes display molecular ion peaks at m/z 331.95 (m+H)+, 348.92 (m+NH4)+, 3591 (m+NH4)+, 328.92 (m+H)+ and 336.76 (m–H)+ respectively, which correspond to the proposed formula weights of the Cobalt, Nickel, Copper, Manganese and Zinc complexes. The peak at 300.03 m/z in the mass spectrum of the Co(II) compound belongs to the metal trimesate, after removing the hydrazine fragment from the complex. The peak at 317.84 m/z is attributed to the cobalt ammonium trimesate fragment. The peak at 630.58 m/z in the mass spectrum of this complex corresponds to the dimer of the compound [Co(Htma)(N2H4)3Co(Htma)] with a hydrazine bridge. Therefore, the mass spectroscopic data complements the analytical results of the elemental (CHN), hydrazine, and metal contents, confirming the proposed molecular formula [M(Htma)(N2H4)2] of the compounds.

Table 1 Analytical data of ligand and complexes

Compound	Molecular weight	Color	Found (calculated)%				
			Carbon (CHN)	Hydrogen (CHN)	Nitrogen (CHN)	Metal (ICP-OES)	Hydrazine
Co(Htma)(N2H4)2	331.15	Light red	32.4(32.6)	8(6)	16.4(16.9)	17.2(17.7)	18.1(19.3)
Cu(Htma)(N2H4)2	335.77	Pale blue	30.1(30.4)	4.3(4.5)	15.5(15.7)	17.5(18.9)	18.4(19.0)
Ni(Htma)(N2H4)2	330.91	Green	30.7(30.9)	4.9(4.5)	16.2(16.0)	16.6(17.7)	18.5(19.3)
Mn(Htma)(N2H4)2	327.16	Dirty white	32.7(301)	1(6)	17.8(17.1)	15.5(16.7)	19.1(19.5)
Zn(Htma)(N2H4)2	337.63	Colorless	31.4(31.9)	5(6)	17.2(16.5)	18.2(19.3)	17.9(18.9)

3.1 Electronic spectra

The character of the ligand field surrounding the metal ion and the shape of the complexes were presumed based on the locations and quantity of d–d bands in the electronic absorption spectral measurements. The electromagnetic spectra of the freshly synthesised cobalt, nickel, and copper compounds, specifically

INTERNATIONAL JOURNAL OF EXPLORING EMERGING TRENDS IN ENGINEERING
Peer-Reviewed, Refereed, Indexed and International Journal, https://ijoeete.com/
|ISSN No. 2394-0573 |Volume: 9, Issue: 01 | January - June 2022

Co(Htma)(N2H4)2, Ni(Htma)(N2H4)2, and Cu(Htma)(N2H4)2, are presented in Fig. 3, showcasing shifts indicative of an octahedral surroundings surrounding these metal cations.

For instance, the cobalt compound exhibits a wide spectrum in the range of 17,500–24,000 cm–1 (λ maximum = 510 nm), which is attributed to the 4T1g (F) → 4T1g (P) shift. The shoulder in this ensemble (approximately 480 nm) might have emerged from the division of the triply degenerate fundamental state (4T1g (F)) caused by spin–orbit interaction. The 4T1g (F) → 4A2g transformation is concealed in the charge-transfer bands in the ultraviolet region, and the 4T1g (F) → 4T2g transformation is anticipated to manifest in the close-infrared region.

The nickel compound displays two spectra, one approximately between 23,000–30,000 cm–1 (λ max = 400 nm) and another approximately between 13,000–14,800 cm–1 (λ max = 722 nm), ascribed to 3A2g → 3T1g (P) (3) and 3A2g → 3T1g (F) (2) transitions, correspondingly. Broadly, octahedral Ni(II) compounds exhibit the 3A2g → 3T2g shift in the near-infrared (NIR) domain. The band at ~655 nm is due to the spin-forbidden 3A2g → 1Eg transition, which gained intensity from the adjacent spin-allowed transition. Based on the noted transition frequencies and the Racah inter-electronic repulsion parameter, B', was computed and determined to be 929 cm–1. This lesser B' value for the compound in comparison to the independent ion B value (1080 for Ni2+), which indicates a covalency factor 'α' (where α = B'/B) for the Ni(II) compound, implies that the metal–ligand connections possess a noteworthy amount of covalent quality. Utilising the B' value, the ligand field partitioning energy 10Dq was computed and was discovered to be 8,305 cm–1.

The copper compound exhibits a spectrum around 12,500–20,408 cm–1, which arises from the 2Eg → 2T2g shift. In a hexacoordinate Cu(II) compound, the eg level of the 2D independent particle basic state will divide into B1g and A1g levels, while the t2g level divides into B2g and Eg levels. Hence, three rotate-permitted changes are anticipated in the observable and nearby-infrared area, but they are exceedingly proximate in energy and frequently manifest in the shape of one extensive band casing.

The Mn(II) and Zn(II) compounds do not exhibit any d-d bands in the visible area, as anticipated for semi- and completely-filled electronic setups of the metallic compounds.

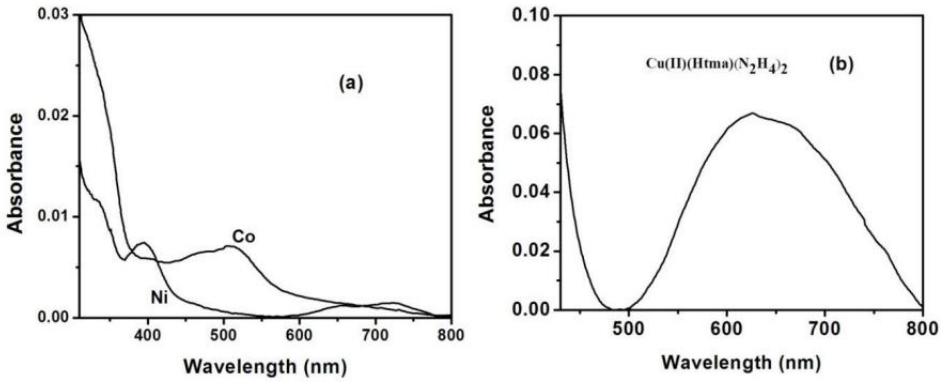

Fig. 2 Electronic Spectra of (a) Co(II)(Htma)(N2H4)2 and Ni(II)(Htma)(N2H4)2, and (b) Cu(II)(Htma)(N2H4)2.

3.2 Infrared spectra

Standard FTIR spectra observed for the compounds Co(Htma)(N2H4)2, Ni(Htma)(N2H4)2, Cu(Htma)(N2H4)2, Mn(Htma)(N2H4)2, and Zn(Htma)(N2H4)2 are exhibited in Fig. 4, and the significant IR absorption wavelengths of the synthesised compounds are enumerated in Table 2. All the arranged complexes exhibit IR bands in the area 3273–3296 cm–1, which are ascribed to N–H stretching frequencies of the hydrazine components. The disproportionate and balanced carboxylate vibrations of all the complexes are observed in the range 1612–1640 and 1363–1372 cm–1, correspondingly, with a Δ between them of 241–277 cm–1, indicating the monodentate coordination of each carboxylate group in the trimesic acid. The N–N oscillation frequency of hydrazine groups detected at 950–985 cm–1 suggests that the hydrazine groups are present as connecting dual-toothed ligands.

INTERNATIONAL JOURNAL OF EXPLORING EMERGING TRENDS IN ENGINEERING
Peer-Reviewed, Refereed, Indexed and International Journal, https://ijoeete.com/
|ISSN No. 2394-0573 |Volume: 9, Issue: 01 | January - June 2022

Table 2 Infrared spectral data (cm–1)

Compound	$\nu_{(N-H)}$	$\nu_{asym(COO^-)}$	$\nu_{sym(COO^-)}$	$\Delta\nu = (\nu_{asym(COO^-)} - \nu_{sym(COO^-)})$	$\nu_{(N-N)}$	$\nu_{(M-O)}$
$Co(Htma)(N_2H_4)_2$	3289	1612	1371	241	983	516
$Ni(Htma)(N_2H_4)_2$	3296	1640	1363	277	979	550
$Cu(Htma)(N_2H_4)_2$	3273	1626	1372	254	985	558
$Mn(Htma)(N_2H_4)_2$	-	1630	1372	258	950	533
$Zn(Htma)(N_2H_4)_2$	3280	1616	1367	249	970	563

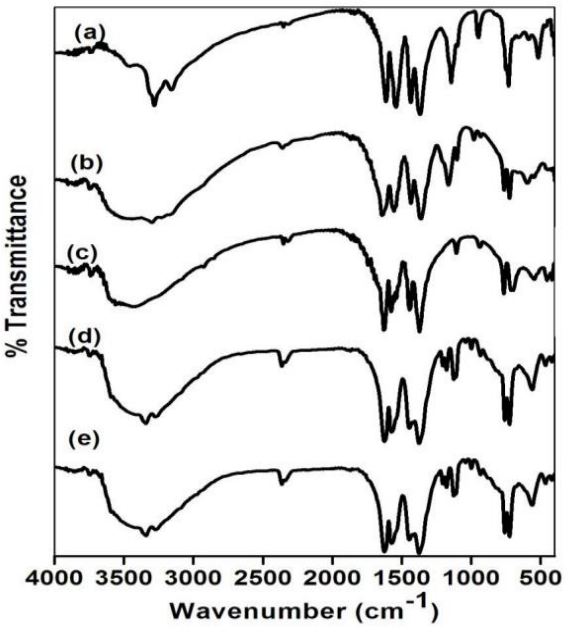

Fig. 3. FTIR spectra of M(Htma)(N2H4)2, where M = (a) Co, (b) Ni, (c) Mn, (d) Cu and (e) Zn.

3.3 Raman spectra

The perceived Raman spectra of metal trimesates and trimesic acid are displayed in Fig. 5. The emblems employed for the different oscillatory patterns are as subsequent: ν represents elongation oscillations, β denotes within-plane flexing patterns, and γ signifies beyond-plane flexing patterns. The infrared and Raman spectroscopic information and their designations are provided in Table

The Raman spectrum of trimesic acid displays the distinctive elongation oscillations of the carbonyl cluster: ν(C=O) at 1648 cm–1, out-of-plane oscillations of the carboxylic cluster: γ(OH)COOH at 955 cm–1, and an elongation oscillation of the hydroxyl cluster (OH)COOH at 3085 cm–1. The spectrums of metal complexes do not display these distinctive bands, which demonstrates that the carboxylate groups are engaged in the coordination with metal. Substitution of the acidic hydrogen with a metallic cation induces a modification in the bond potencies of carboxylate clusters and additionally brings about a depletion of intermolecular hydrogen bonding, resulting in noticeable alterations in the infrared and Raman spectra of the metallic trimesates in comparison to those of trimesic acid.

For example, the bands caused by carboxylic group oscillations vanished in the complexes, while peaks originating from carboxylate anion oscillation are evident. In trimesic acid, the spectrum that arises from out-

INTERNATIONAL JOURNAL OF EXPLORING EMERGING TRENDS IN ENGINEERING
Peer-Reviewed, Refereed, Indexed and International Journal, https://ijoeete.com/
|ISSN No. 2394-0573 |Volume: 9, Issue: 01 | January - June 2022

of-plane flexing modes of the ring double bond and a carboxylic group, γ(C=C)—c=c—, is observed at approximately 998 cm–1. This group is relocated towards elevated wavenumbers (approximately 1000 cm–1) in the spectra of compounds, indicating an increased electronic charge density surrounding the dual linkage (—C=C—) in trimesates compared to trimesic acid.

The bands perceived in the areas of ~1425 cm–1 and ~1590 cm–1 are caused by the elongation oscillations of the fragrant circle. These groups emerged at approximately equivalent wavenumbers both in the spectrum of trimesic acid and in the compounds. This implies that the fragrant system has not been disturbed significantly upon coordination of trimesic acid with metals through carboxylate groups.

Table 3 Raman spectral data (cm–1)

Assignments of selected bands (cm–1) occurring in the IR and Raman spectra of trimesic acid and cobalt(II), nickel(II), manganese(II), copper(II) and zinc(II) trimesates.

Trimesic acid		Co(Htma)(N2H4)2		Ni(Htma)(N2H4)2		Mn(Htma)(N2H4)2		Cu(Htma)(N2H4)2		Zn(Htma)(N2H4)2		Assignment
IR	Raman	IR	Raman	IR	Raman	IR	Raman	IR	Raman	IR	Raman	
3085 vw	3077 w	-	-	-	-	-	-	-	-	-	-	(OH)COOH
1712 s	1648 s	-	-	-	-	-	-	-	-	-	-	(C=O)
-	-	1612 s	1596 m	1640 s	1609 m	1614 s	1631 s	1626 s	1605 m	1616 vs	1580 m	- as(COO)
1607 m	-	1523 vs	1545 m	1554 s	1554 m	1583 vs	-	1577 s	1545 w	1577 vs	-	(CC)ar
1455 s	1424 m	1435 vs	1420 s	1436 s	1449 s	1445 vs	1457 vs	1437 vs	1432 m	1442 s	1457 s	(CC)ar
-	-	1371 vs	1392 m	1363 vs	1365 m	1372 s	1363 w	1372 vs	1363 vw	1367 vs	1364 m	- s(COO)
1112 s	-	1151 m 1113 vw	1101 vw	1165 vs 1101 m	1061 m	1106 s	1155 vw	1181 vw	1097 s	1176 vw 1108 s	1171 vw	ß(CH)
955 vw	-	-	-	-	-	-	-	-	-	-	-	γ(OH)COOH
-	1000 vs	-	1001 vs	-	1002 vs	-	1002 vs	1007 m	998 vs	1002 w	1002 vs	γ(CH)-C=C-

Note: vs – very strong, s – strong, m – medium, w – weak, vw – very weak.

INTERNATIONAL JOURNAL OF EXPLORING EMERGING TRENDS IN ENGINEERING
Peer-Reviewed, Refereed, Indexed and International Journal, https://ijoeete.com/
|ISSN No. 2394-0573 |Volume: 9, Issue: 01 | January - June 2022

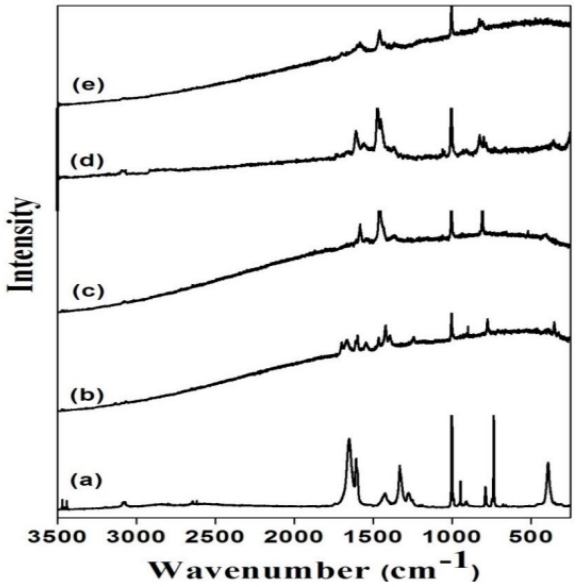

Fig. 4. Raman spectra of trimesic acid (a) and trimesates complexes of cobalt (b), nickel (c), manganese (d) and zinc (e).

3.4 EPR spectra

EPR spectra of solid samples of the compounds under investigation were recorded at ambient temperature. The specimens demonstrate EPR signals characteristic of the solitary entity with vertical symmetry. Illustrative EPR spectra of cobalt(II), copper(II), nickel(II), and manganese(II) compounds (solid specimen) at room temperature are depicted in Figure 6. The g‖ and g⊥ values were obtained from the EPR spectra of complexes using 2,2-diphenyl-1-picrylhydrazyl (DPPH) free radical as 'g' indicator and the acquired g values are showcased in Table 4. The EPR spectra exhibit lack of hyperfine splitting, which could be attributed to the circumstance that the paramagnetic centre is not diluted. For the copper compound, the detected g‖ magnitude (2.261) is greater than the g⊥ magnitude (1.834) indicating that the solitary electron is concentrated in the dx2−y2 orbital of the metal ions. It is in harmony with the reality that, for d9 system in deformed octahedral structure the solitary electron resides in the dx2−y2 orbital providing 2B1g as the fundamental state with g parallel > g perpendicular.

In accordance with Kivelson and Neiman,[21] the g value of < 2.3 suggests covalent quality of the metal–ligand bond and >2.3 signify ionic quality. Utilising these criteria to the 'g' values perceived for the complexes (Table 4), a covalent nature for the metal–ligand connection in the complexes under examination has been foreseen which is in accordance with the electronic spectral findings. According to Hathaway and Billing,[22] if the minimum g > 2.04 (either g‖ or g⊥) and G (defined as G = (g‖ − 2)/(g⊥ − 2)) is lower than 4, (i.e., g > 2.04 and G < 4) there is a noteworthy interchange interaction in the solid complexes; if the minimum g < 2.03, the metal ion may be in compressed tetragonal-octahedral stereochemistry. The patterns g⊥< ge (2.0023) < g‖ and the g⊥< 2.03 (g⊥ is minimum g in these compounds) observed for Co(II), Ni(II) and Cu(II) compounds imply that there is no interchange interaction in the solid compounds and these compounds have axially compressed octahedral structure.[22,23]

Table 4 EPR spectral data of the prepared complexes

Complex	g‖	g⊥	giso
Co(Htma)(N2H4)2	2.217	1.842	1.967
Ni(Htma)(N2H4)2	2.279	1.894	2.02
Mn(Htma)(N2H4)2	–	–	1.987
Cu(Htma)(N2H4)2	2.261	1.834	2.02

INTERNATIONAL JOURNAL OF EXPLORING EMERGING TRENDS IN ENGINEERING
Peer-Reviewed, Refereed, Indexed and International Journal, https://ijoeete.com/
|ISSN No. 2394-0573 |Volume: 9, Issue: 01 | January - June 2022

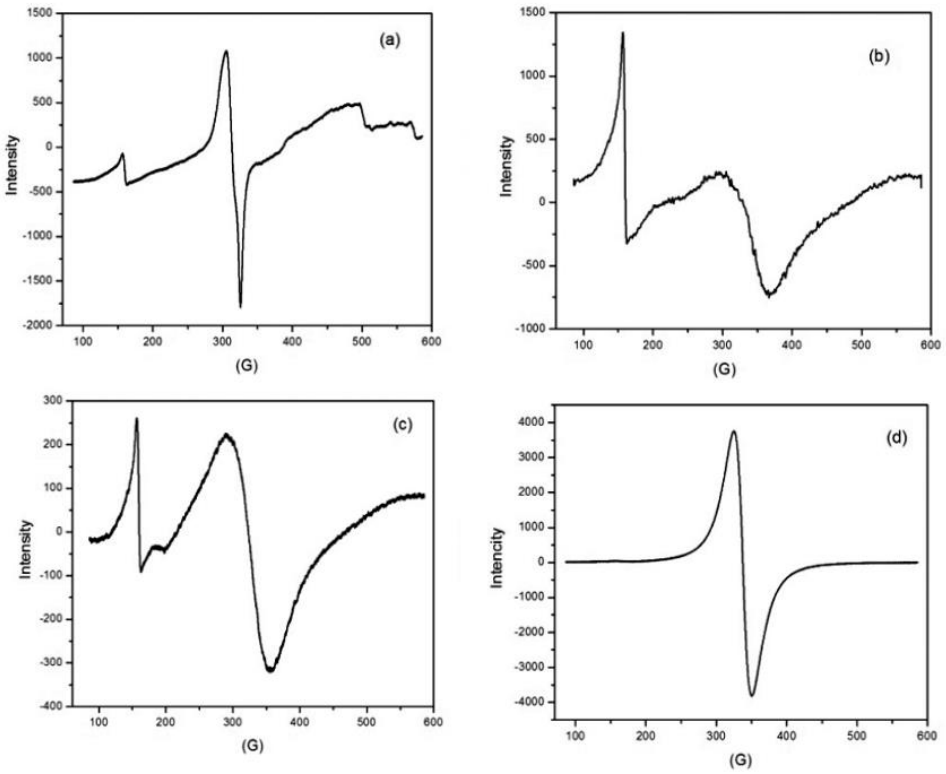

Fig. 5. EPR spectra of (a) Cu(II), (b) Co(II), (c) Ni(II) and (d) Mn(II) Complexes at RT.

3.5 Thermal decomposition studies

The concurrent TG–DTA diagrams of cobalt, copper, manganese, nickel and zinc compounds are displayed in Fig. 7 and the calorimetric data are provided in Table 5. By fitting the observed mass losses in TG with potential decomposition products, the compositions of the intermediates and the ultimate products were obtained.[Twenty-four to thirty-four] The TG tracings of all the formulated compounds, M(Htma)(N2H4)2 where M = Cobalt, Nickel, Manganese, Copper and Zinc, exhibit three-stage degradation in accordance with DTA revealing either heat-absorbing or heat-releasing changes. In the preliminary phase, the compounds of Manganese, Nickel, and Zinc disintegrate exothermically at 85–290 °C with a weight reduction corresponding to two particles of hydrazine to yield the corresponding metal hydrogen trimesate as an intervening substance. However, the intricate combination of Cobalt and Copper disintegrate in an energetically demanding manner to shed a single hydrazine molecule during the initial phase, resulting in the formation of metal hydrazine hydrogen trimesate as an intervening substance. In the subsequent phase, the middle disintegrate (310–420 °C) to shed the organic components and produce the corresponding metal carbonates as the subsequent middle stage. In the ultimate phase, the metal carbonate intermediate additionally breaks down to generate corresponding metal oxide as the ultimate outcome.

Table 5 Thermal data

Complexes	DTA Temp./°C	Thermogravimetry (TG)		Decomposition products
		Temp. range/°C	Mass loss/% Found(Calculated)	
Co(Htma)(N2H4)2	168(+)	73-236	8.3(9.6)	Co(Htma).N2H4
	331(+)	236-511	55.2(54.3)	CoCO3
	541(+)	511-857	15.7(12)	CoO
	124(+)	66-165	10.4(9.5)	Cu(Htma)(N2H4)

INTERNATIONAL JOURNAL OF EXPLORING EMERGING TRENDS IN ENGINEERING
Peer-Reviewed, Refereed, Indexed and International Journal, https://ijoeete.com/
|ISSN No. 2394-0573 |Volume: 9, Issue: 01 | January - June 2022

Cu(Htma)(N2H4)2	237(+) 354(-)	165-282 282-538	8.2(9.5) 58(54.2)	Cu(Htma) CuO
Mn(Htma)(N2H4)2	168(+) 560(+) 947(-)	44-313 313-656 656-979	20.1(19.5) 44.5(45.2) 11(14)	Mn(Htma) $MnCO_3$ MnO
Ni(Htma)(N2H4)2	177(+) 297(+) 608(+)	82-269 269-539 539-931	18.8(19.3) 45.1(44.7) 14.5(12)	Ni(Htma) $NiCO_3$ NiO
Zn(Htma)(N2H4)2	150(+) 415(-) 685(+)	51-287 287-631 631-970	18.1(18.9) 42.5(48) 18(14.2)	Zn(Htma) $ZnCO_3$ ZnO

Note: (+) Endo thermic decomposition (-) Exo thermic decomposition

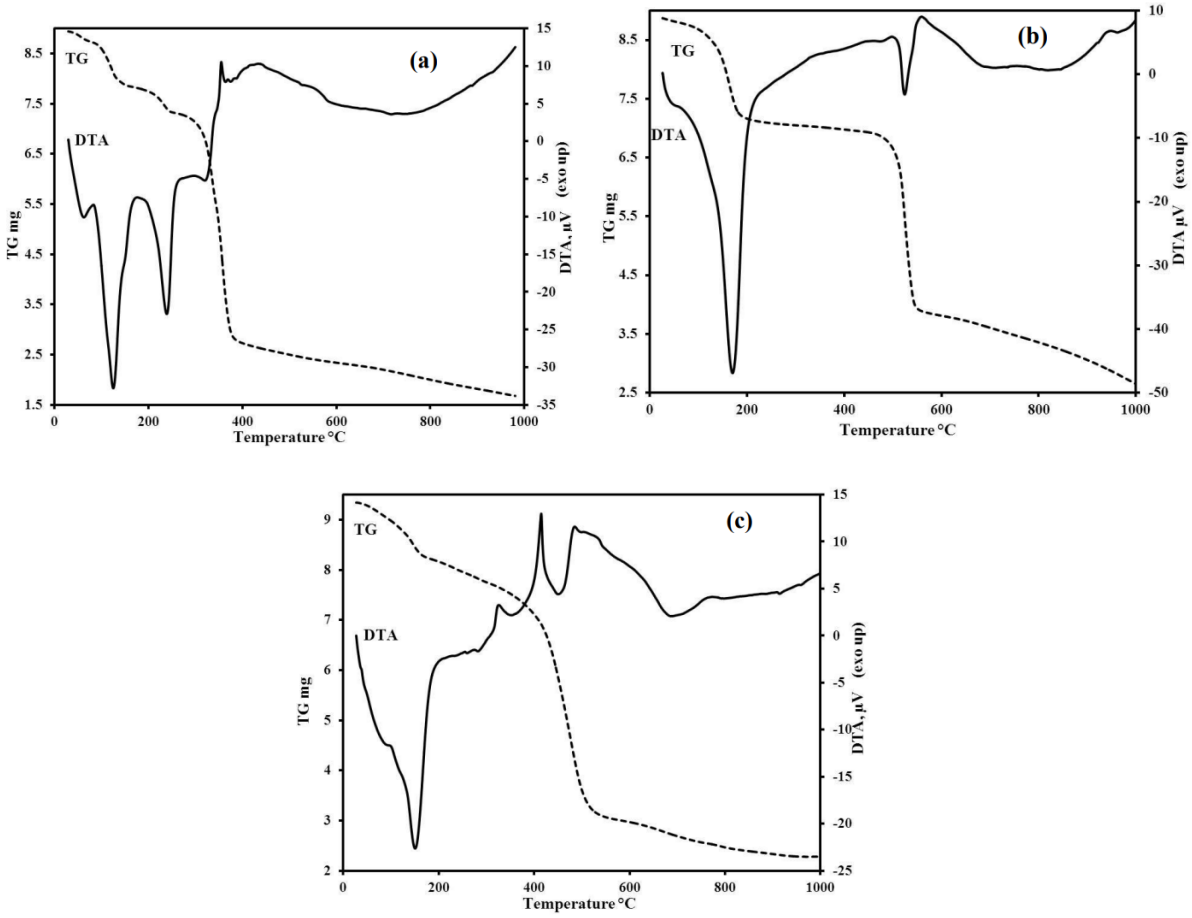

Fig. 6. Simultaneous TG–DTA curves of (a) Cu(Htma)(N2H4)2, (b) Mn(Htma)(N2H4)2 and (c) Zn(Htma)(N2H4)2.

3.6 Powder X-ray diffraction

INTERNATIONAL JOURNAL OF EXPLORING EMERGING TRENDS IN ENGINEERING
Peer-Reviewed, Refereed, Indexed and International Journal, https://ijoeete.com/
|ISSN No. 2394-0573 |Volume: 9, Issue: 01 | January - June 2022

The documented powder X-ray diffraction patterns of the compounds are displayed in Fig. 8. A juxtaposition of the XRD data of distinct complexes discloses that all the complexes display analogous XRD patterns, suggesting that the crystal structures of these complexes are congruous with one another. The summits detected at 2θ angles of 10.37°, 20.86°, 38.1°, and 42.39° for the Mn compound can be identified, correspondingly, to the (1 0 0), (2 0 0), (3 2 0), and (4 0 0) planes of the uncomplicated cubic crystal configuration.

X-ray diffraction (XRD) patterns of Co(II), Ni(II), Cu(II), and Zn(II) compounds are quite comparable, and all these compounds display peaks at 2θ angles of approximately 11.4°, 18.1°, and 26.0°, corresponding, respectively, to the (1 1 0), (2 1 0), and (3 1 0) planes of a tetragonal crystal lattice. The magnitude of all the peaks is quite low, and less distinct patterns are observed in the 2θ range of 45–70°, indicating that the complexes might possess a polymeric arrangement or primarily amorphous character. Efforts to ready solitary crystals were not fruitful.

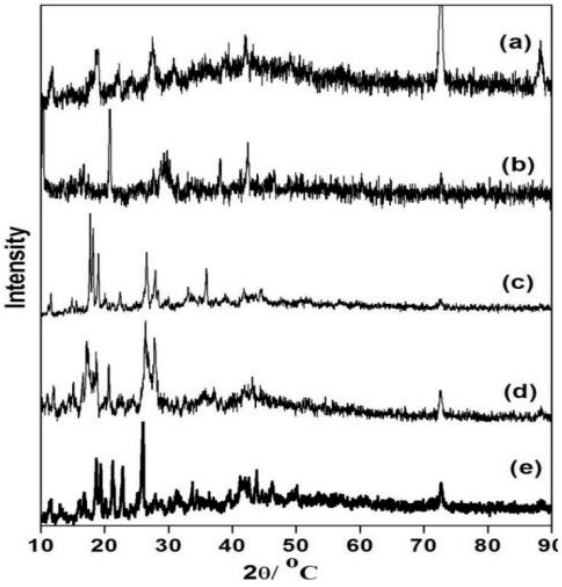

Fig. 7. Powder XRD patterns of the complexes M(Htma)(N2H4)2, where M = (a) Co, (b) Mn, (c) Ni, (d) Zn and (e) Cu.

7 SEM and EDAX studies

The compounds were incinerated in a kiln at their decomposition temperature and heated at 800 °C for 1 h to obtain the oxides of the elements, and subsequently, the structure and particle size of the oxides produced were examined. The SEM pictures of remnants acquired from Cu(Htma)(N2H4)2 and Mn(Htma)(N2H4)2 are displayed in Fig. 9 and the EDX diagrams obtained for these remnants (oxides) are provided in Fig. 10.

INTERNATIONAL JOURNAL OF EXPLORING EMERGING TRENDS IN ENGINEERING
Peer-Reviewed, Refereed, Indexed and International Journal, https://ijoeete.com/
|ISSN No. 2394-0573 |Volume: 9, Issue: 01 | January - June 2022

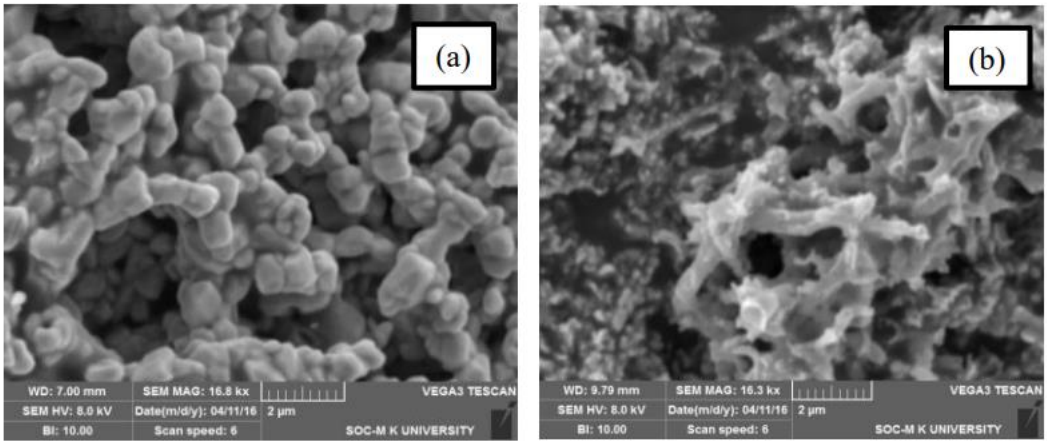

Fig. 8. SEM images of (a) CuO and (b) MnO obtained using Cu(Htma)(N2H4)2 and Mn(Htma)(N2H4)2 complexes.

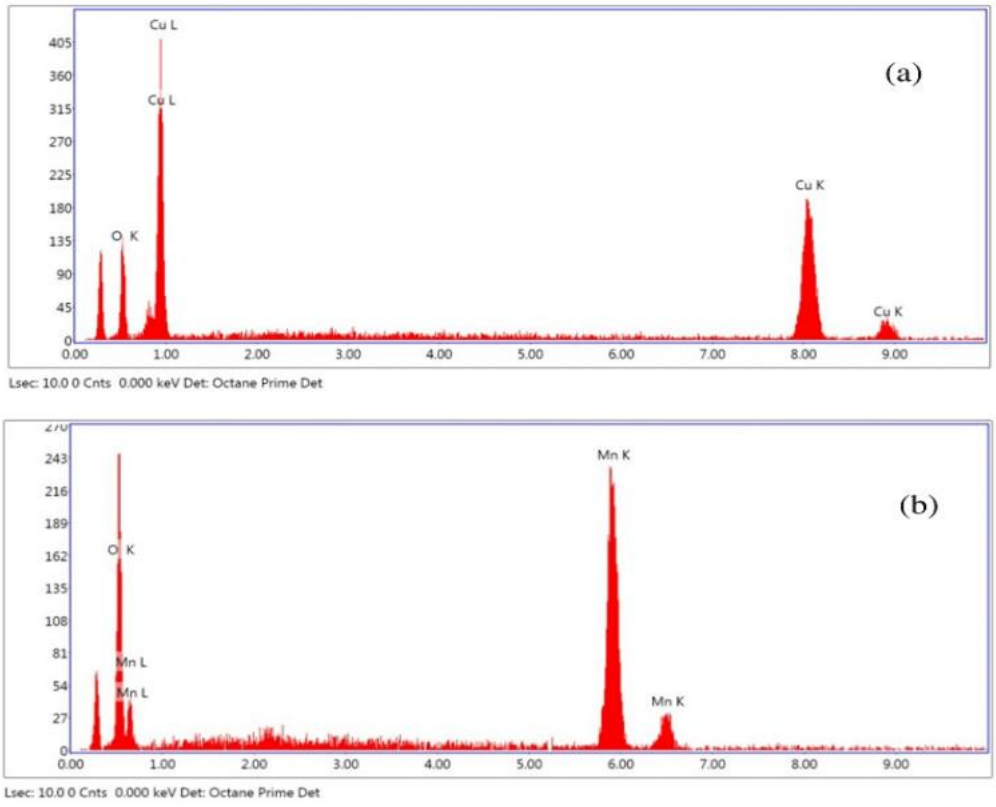

Fig. 9. EDX spectra of (a) CuO and (b) MnO obtained using Cu(Htma)(N2H4)2 and Mn(Htma)(N2H4)2 complexes.

INTERNATIONAL JOURNAL OF EXPLORING EMERGING TRENDS IN ENGINEERING
Peer-Reviewed, Refereed, Indexed and International Journal, https://ijoeete.com/
|ISSN No. 2394-0573 |Volume: 9, Issue: 01 | January - June 2022

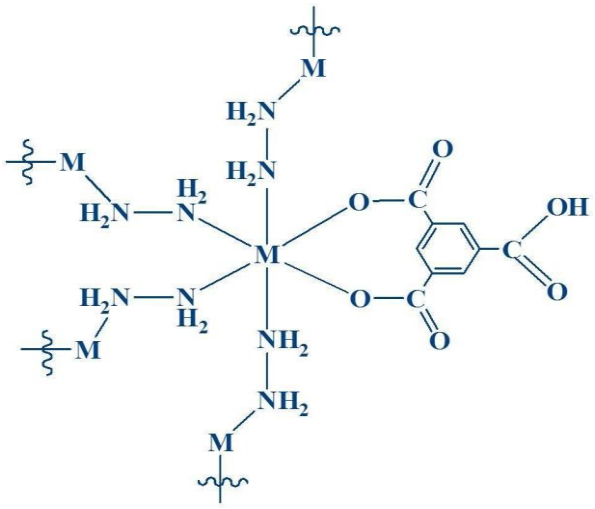

Fig. 10. Proposed structure of M(Htma)(N2H4)2 where M = Co, Ni, Cu, Mn and Zn.

3.8 Antimicrobial Activities

3.8.1 Antibacterial activity studies

The antibacterial actions of the ligand and the complexes of Mn(II), Co(II), Ni(II), Cu(II) and Zn(II) were checked on three Gram-negative bacteria viz., Pseudomonas aeruginosa, Proteus mirabilis and Vibrio harveyi and a Gram-positive bacterium Staphylococcus aureus by the disc diffusion technique. The zone of inhibition around each disk, after incubation, was measured in millimeter and presented in Fig. 12 and Table 6. It is clear from Fig. 12 that the growth inhibitions are much larger by metal complexes than by the bare ligand. The enhanced activity of the metal complexes can be explained on the basis of chelation theory.[38] The chelation tends to make the ligands act as more powerful and potent bactericidal agents, thus inhibits bacteria growth more than the bare ligand. The Zn(II) complex showed remarkable activity against P. mirabilis, S. aureus and P. aeruginosa than other complexes. The Co(II) complex is highly active against P. aeruginosa microorganism. The Mn(II) complex has very low activity against all the four microorganisms.

Table 6 Antibacterial activity results of ligand and its metal complexes

Compound (1 mg/mL)	Growth Inhibition against Bacteria (diameter in mm)			
	P. aeruginosa	P. mirabilis	V. harveyi	S. aureus
H3tma	3	5	4	3
Co(Htma)(N2H4)2	26	10	9	10
Ni(Htma)(N2H4)2	10	-	10	10
Cu(Htma)(N2H4)2	12	10	12	12
Mn(Htma)(N2H4)2	-	-	-	-
Zn(Htma)(N2H4)2	20	16	14	32
Streptomycin (Std)	38	34	36	34

INTERNATIONAL JOURNAL OF EXPLORING EMERGING TRENDS IN ENGINEERING
Peer-Reviewed, Refereed, Indexed and International Journal, https://ijoeete.com/
|ISSN No. 2394-0573 |Volume: 9, Issue: 01 | January - June 2022

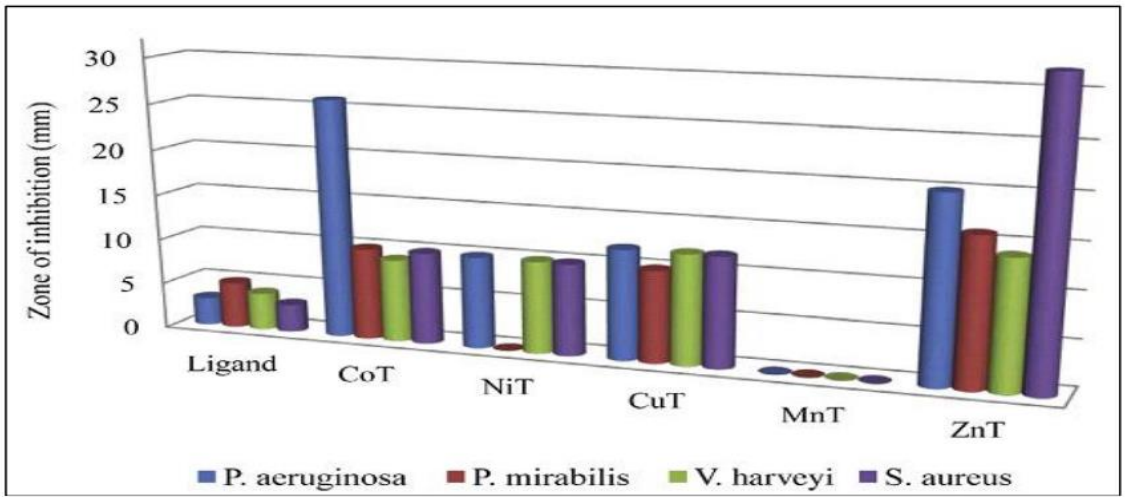

Fig. 11. Antibacterial activity of the ligand and complexes.

8.2 In vitro antifungal activity

In vitro antifungal activities of trimesic acid (H3tma) and its metal complexes were carried out against four fungi Candida albicans, Aspergillus niger, Aspergillus fumigatus and Penicilium variance and compared with standard antifungal drug Ketoconazole at the same concentration. Antifungal activity data are given in Table 7 and the mycelial growth of inhibition are presented in Fig. 13 and Fig. 14. The antifungal activity data showed hydrazine with transition metal complexes are more active compared than the free ligand. All the metal hydrazine complexes showed highly remarkable antifungal activity against the entire microorganism as compared to the activity of the reference drug Ketoconazole. Among all the prepared complexes, the complexes of Cu(Htma)(N2H4)2 and Zn(Htma)(N2H4)2 were the maximum active against all the tested fungi and exhibited the Zn(II) complex a greater activity (22mm) against P. variance. The effective antifungal activity of synthesized complexes compared to the corresponding ligand can be explained on the basis of chelation theory. The polarity of the metal ion will be reduced to a greater extent upon chelation due to the overlap of the ligand orbital and partial sharing of the charge of the metal ion with donor groups. It increases the delocalization of π-electrons over the whole chelating ring and enhances the penetration of the complexes into lipid membranes and block the metal binding sites in the enzymes of microorganisms. Thus, these complexes disturb the respiration process of the cell and block the synthesis of proteins, which restricts further growth of microorganism.[39]

Table 7 In vitro antifungal screening data of the ligand, its metal complexes and the standard drug

Compounds (1 mg/mL)	Mycelial growth inhibition in mm			
	A. fumigatus	A. niger	P. variance	C. albicans
H3tma	12	8	11	10
Co(Htma)(N2H4)2	17	13	17	18
Ni(Htma)(N2H4)2	20	13	21	16
Cu(Htma)(N2H4)2	20	15	20	20
Mn(Htma)(N2H4)2	19	12	17	19
Zn(Htma)(N2H4)2	19	15	22	18
Ketoconazole (Std)	23	16	24	21

INTERNATIONAL JOURNAL OF EXPLORING EMERGING TRENDS IN ENGINEERING
Peer-Reviewed, Refereed, Indexed and International Journal, https://ijoeete.com/
|ISSN No. 2394-0573 |Volume: 9, Issue: 01 | January - June 2022

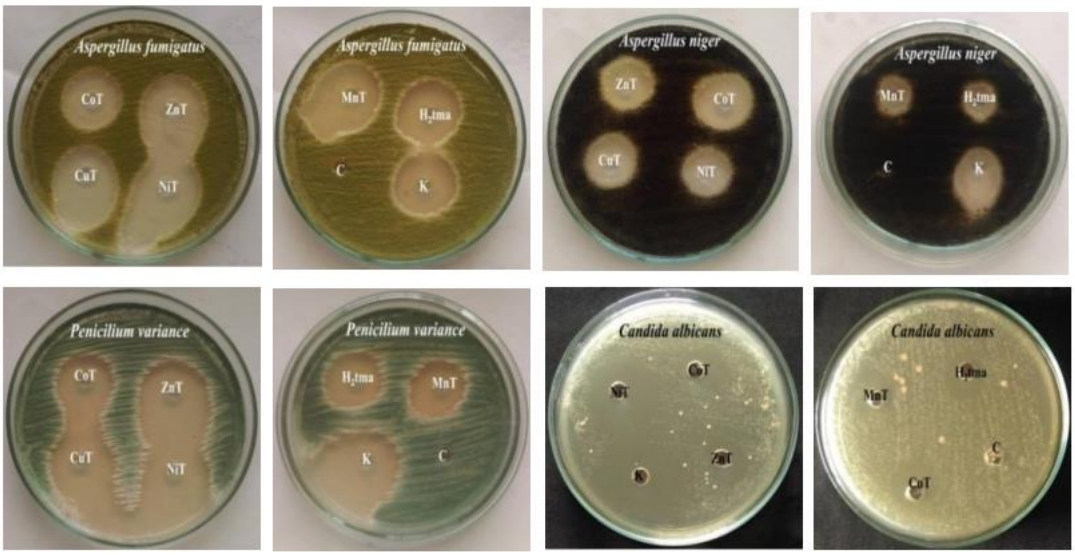

Fig. 12 Antifungal action of ligand and metal complexes (well diffusion method).

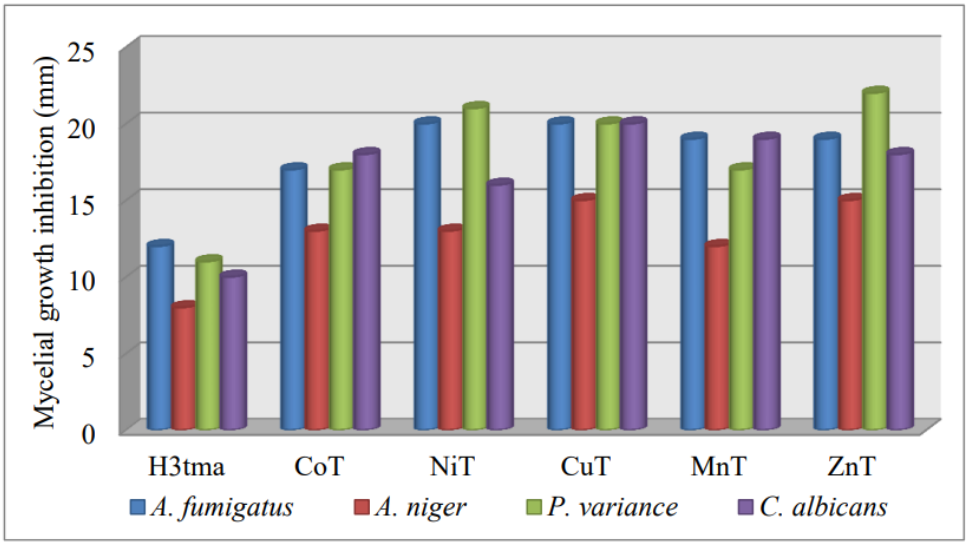

Fig. 13. Antifungal activity of the ligand and complexes.

9. Conclusions

The new trimesic acid/hydrazine mixed-ligand complexes of Mn2+, Co2+, Ni2+, Cu2+ and Zn2+ contain hydrazine molecule as a bridging bidentate. The 1,3,5-benzenetricarboxylate ion is acting as bidentate, through bonding of two carboxylate groups (each acting as a monodentate) to metal ion. A compressed tetragonal-octahedral stereochemistry for the metal ions in the complexes has been deduced from the UV–vis absorption and EPR spectral studies. The complexes are isolated only as powders and the featureless XRD pattern in the 2 range of 45–70° and their sparingly soluble nature suggest a polymeric structure. The complexes could be used as a precursor for nano-metal oxides preparation. The newly prepared metal complexes exhibited decent antibacterial and antifungal activity when compared to the corresponding metal free ligand. From the entire complexes, the Cobalt(II) and zinc(II) complexes display good antibacterial activity against P. aeruginosa and S. aureus on comparing with standard drug (Streptomycin). Among all the newly synthesized complexes, the complexes of Cu(II) and Zn(II) showed very good antifungal activity against the four tested fungi on compared with reference drug (Ketoconazole).

θ

References

1. J.W. Steed, J.L. Atwood, Supramolecular Chemistry, second ed., Wiley, New York, 2000.
2. J.P. Sauvage, Transition Metals in Supramolecular Chemistry, 5, Wiley, New York, 1999.
3. A.R. Millward, O.M. Yaghi, J. Am. Chem. Soc. 127 (2005) 17998–17999.
4. A.Muller, Y. Zhou, H. Bogge, M. Schmidtmann, T. Mitra, E.T.K. Haup, A. Berkle, Angew. Chem. Int. Ed. 45 (2006) 460–465.
5. B.N. Sivasankar, S. Govindarajan, Synth. React. Inorg. Met.-Org. Chem. 24 (1994) 1573–1582.
6. B.N. Sivasankar, S. Govindrajan, Synth. React. Inorg. Met.-Org. Chem. 24 (1994) 1583–1597.
7. T. Premkumar, S. Govindarajan, J. Therm. Anal. Calorim. 100 (2010) 725– 732.
8. L. Vikram, B.N. Sivasankar, J. Therm. Anal. Calorim. 91 (2008) 963–970.
9. L.R. Gonsalves, V.M.S. Verenkar, S.C. Mojumdar, J. Therm. Anal. Calorim. 96 (2009) 53–57.
10. Z. Rzqczynska, A. Ostasz, S. Pikus, J. Therm. Anal. Calorim. 82 (2005) 347– 351.
11. F. Ying, L. Guobao, L. Fuhui, X. Ming, L. Jianhua, J. Mol. Struct. 1004 (2011) 252–256.
12. C. Zhenfeng, R. Huijuan, L. Guixia, H. Guangyan, J. Rare Earths 24 (2006) 724–727.
13. J.X. Chen, S.X. Liu, E.Q. Gao, Polyhedron 23 (2004) 1877–1888.
14. A.B.P. Lever, Inorganic Electronic Spectroscopy, 2nd ed., Elsevier, Amsterdam, 1894.
15. A.B.P. Lever, J. Chem. Educ. 45 (11) (1968) 711.
16. K. Nakamoto, Infrared and Raman Spectra of Inorganic and Coordination Compounds, Wiley, New York, 1978.
17. A.Braibanti, F. Dallavalle, M.A. Pellingheli, E. Laporati, Inorg. Chem. 7 (1968) 1430–1433.
18. G. Varsanyi, M.A. Kovner, L. Lang, Assignments for Vibrational Spectra of 700 Benzene Derivatives, Akademia Kiado, Budapest, 1973.
19. M. Kalinowska, J. Piekut, A. Bruss, C. Follet, J.S. Gromiuk, R. Swislocka, Z. Rzaczynska, W. Lewandowski, Spectrochim. Acta A 122 (2014) 631–638.
20. S.X. Min, W.H. Yan, L.Y. Bing, Y.J. Xiu, C. Lei, H. Ge, X.W. Qing, Z. Bing,
21. Chem. Res. Chin. Univ. 26 (2010) 1011–1015.
22. D. Kivelson, R. Neiman, J. Chem. Phys. 35 (1961) 149.
23. B.J. Hathaway, D.E. Billing, Coord. Chem. Rev. 5 (1970) 143–207.
24. B.J. Trzebiatowska, J. Lisowski, A. Vogt, P. Chemielewski, Polyhedron 7 (1988) 337–343.
25. V. Jordanovska, R. Trojko, Thermochim. Acta 258 (1995) 205–217.
26. H. Icbudak, T.K. Yazicilar, V.T. Yilmaz, Thermochim. Acta 335 (1999) 93– 98.
27. U.B. Gawas, V.M.S. Verenkar, Thermochim. Acta 556 (2013) 41–46.
28. K. Saravanan, S. Govindarajan, D. Chellappa, Synth. React. Inorg. Met.-Org. Chem. 34 (2004) 353–369.
29. S. Yasodhai, S. Govindarajan, Synth. React. Inorg. Met.-Org. Chem. 29 (1999) 919–934.
30. B.N. Sivasankar, S. Govindarajan, Mater. Res. Bull. 31 (1996) 47–54.
31. K. Saravanan, S. Govindarajan, J. Chem. Sci. 114 (2002) 25–36.
32. T. Premkumar, S. Govindarajan, Thermochim. Acta 386 (2002) 35–42.
33. S. Vairam, T. Premkumar, S. Govindarajan, J. Therm. Anal. Calorim. 100 (2010) 955–960.
34. K. Kuppusamy, S. Govindarajan, Thermochim. Acta 274 (1996) 125–138.
35. S. Vairam, T. Premkumar, S. Govindarajan, J. Therm. Anal. Calorim. 101
36. (2010) 979–985.
37. L. Vikram, B.N. Sivasankar, Thermochim. Acta 452 (2007) 20–27.
38. S. Yasodhai, S. Govindarajan, J. Therm. Anal. Calorim. 62 (2000) 737–745. 37.
39. K.C. Patil, J. Chem. Sci. 96 (1986) 459–464.
40. B.G. Tweedy, Phytopathology 55 (1964) 910–914.
41. N. Dharmaraj, P. Viswanathamurthi, K. Natarajan, Trans. Met. Chem. 26 (2002) 105–109.